

Article

# Potentiometric Sensor Based on Layered Pillar[6]arene—Copper Composite

Michail Sorvin<sup>1</sup>, Guzeliya Galimzyanova<sup>1</sup>, Vladimir Evtugyn<sup>2</sup>, Alexey Ivanov<sup>1</sup>, Dmitry Shurpik<sup>1</sup>, Ivan Stoikov<sup>1</sup> and Gennady Evtugyn<sup>1,3,\*</sup>

<sup>1</sup> A.M. Butlerov' Chemistry Institute, Kazan Federal University, 18 Kremlevskaya Street, Kazan 420008, Russia

<sup>2</sup> Interdisciplinary Center of Analytical Microscopy, Kazan Federal University, 18 Kremlevskaya Street, Kazan 420008, Russia

<sup>3</sup> Analytical Chemistry Department, Chemical Technology Institute, Ural Federal University, 19 Mira Street, Ekaterinburg 620002, Russia

\* Correspondence: gennady.evtugyn@kpfu.ru

**Abstract:** A solid-contact potentiometric sensor has been developed on the basis of glassy carbon electrode covered with electropolymerized polyaniline and alternatively layered pillar[6]arene and Cu<sup>2+</sup> ions films. The assembly of the surface layer was confirmed by surface plasmon resonance measurements. The number of deposited layers was selected to reach better analytical characteristics for Cu<sup>2+</sup> determination. It was shown that better results were achieved by using five layers, the upper one consisting of the macrocycle. The addition of covering layers for polyelectrolytes (Nafion, poly(styrene sulfonate)) and Cu<sup>2+</sup> ions did not improve sensor performance. The potentiometric sensor made it possible to determine Cu<sup>2+</sup> ions in neutral and weakly acidic media with a linear range of the concentrations, from 3.0 μM to 10.0 mM (limit of detection 3.0 μM). The applicability of the sensor in real sample assays was confirmed by the determination of Cu<sup>2+</sup> ions in copper vitriol, Bordeaux mixture, and polyvitamin-mineral pills of “Complivit” during an atomic emission spectroscopy analysis.

**Keywords:** solid-contact sensor; potentiometric sensor; pillar[6]arene; polyaniline; copper determination



**Citation:** Sorvin, M.; Galimzyanova, G.; Evtugyn, V.; Ivanov, A.; Shurpik, D.; Stoikov, I.; Evtugyn, G. Potentiometric Sensor Based on Layered Pillar[6]arene—Copper Composite. *Chemosensors* **2023**, *11*, 12. <https://doi.org/10.3390/chemosensors11010012>

Academic Editor: Gabriela Broncová

Received: 23 November 2022

Revised: 16 December 2022

Accepted: 19 December 2022

Published: 22 December 2022



**Copyright:** © 2022 by the authors. Licensee MDPI, Basel, Switzerland. This article is an open access article distributed under the terms and conditions of the Creative Commons Attribution (CC BY) license (<https://creativecommons.org/licenses/by/4.0/>).

## 1. Introduction

Solid-contact potentiometric sensors offer new opportunities of further progress in potentiometry thanks to the obvious advantages that they possess, i.e., flexible design, miniaturization prospects, durability, low-cost manufacturing, and the variety of the materials introduced [1–3]. The elimination of internal filling applied in conventional ion-selective electrodes with plastic membranes makes it possible to avoid leaching in the internal standard solution, which is considered as a main weak point of such sensors. Direct contact of the ionophore with the transducer requires implementing the intermediate material with mixed electronic and ionic conductivity, which compensates for charge changes on the electrode interface and converts ion transfer into the electron flow, followed by electromotive force measurement. Oxides and complexes of transition metals and conducting polymers can be introduced as ion-to-electrode transducer prior to the deposition of ionophore-containing film. Thus, polyaniline, polypyrrole, and polythiophene derivatives have been described in the assembly of the solid-contact sensors for the determination of metal cations [4–10], inorganic anions [11,12], and organic species [13–16]. The use of electroconductive polymers in the potentiometric sensors can be limited by the low reversibility of the redox reactions within the surface layer. This can be improved by the additional implementation of metal nanoparticles or mediators of electron transfer. Complications in the surface-layer content call for the optimization of the assembling protocol, which can involve the introduction of auxiliary agents in the electropolymerization media, the

physical adsorption of appropriate components, and the use of supramolecular assembling for the reactants prior to polymer deposition or on the polymer film surface [17–19].

Pillararenes are a new class of macrocyclic molecules made up of hydroquinone units linked with methylene bridges at *para* position [20]. Pillararenes show complexation properties toward various cationic species (paraquat [21], Na<sup>+</sup>/K<sup>+</sup> [22], Ag<sup>+</sup> ions [23], pH [24]), which can be modified by the introduction of various substituents at hydroxyl groups of the macrocycle. Recently, the cross-selectivity of partially substituted pillar[5]arenes has been investigated for a series of alkali-, alkali-earth, and transient metal cations [25]. However, all these examples are related to the use of pillar[5]arene derivatives. Meanwhile the use of pillar[6]arene (P[6]A) remains underestimated and is mostly located by fluorescent sensors with substituted macrocycles involved in host–guest complexation with guest species [26]. In comparison with pillar[5]arene, whose activity is complicated by intramolecular bonds affecting its redox reactions [27], P[6]A exerts the independent oxidation of hydroquinone units and the reversed reduction of quinone fragments formed on the electrode interface [28]. Together with a bigger cavity and a more flexible structure, this offers new opportunities for assembling appropriate potentiometric sensors.

In this work, the design of the potentiometric sensor obtained by the consecutive deposition of P[6]A and Cu<sup>2+</sup> ions onto the polyaniline support has been investigated and the performance of appropriate sensors for Cu<sup>2+</sup> determination explored.

## 2. Materials and Methods

### 2.1. Reagents

Aniline, CuCl<sub>2</sub>·2H<sub>2</sub>O, hydroquinone, potassium hexacyanoferrate (III) (99%), potassium hexacyanoferrate (II) (98.5–102%), 11-mercaptoundecanoic acid (MUA), sodium poly(4-styrene sulfonate) (PSS, average mol. mass 1 MDa), poly(allylamine) (PAA, average mol. mass 65 kDa), and poly(diallyldimethylammonium chloride) (PDDA, mol. mass 400,000–500,000) were purchased from Sigma-Aldrich (Darmstadt, Germany) and Nafion 117 (5% in the mixture of lower aliphatic alcohols and water) from Merck (Darmstadt, Germany). Other reagents were of analytical grade.

Copper vitriol, Bordeaux mixture, and polyvitamin drops of “Complivit” (UfaVita, Russia) were purchased in a local market. “Complivit” contained vitamins A, B, C, and E, and minerals (2.5 mg of FeSO<sub>4</sub>, 2.9 mg of CuSO<sub>4</sub>, 217 mg of CaHPO<sub>4</sub>, 0.4 mg of CoSO<sub>4</sub>, 117 mg of MgHPO<sub>4</sub>, 11 mg of MnSO<sub>4</sub>, and 8.8 mg of ZnSO<sub>4</sub> per one pill). All the solutions were prepared with Millipore Q water (Simplicity water purification system, Merck-Millipore, France). Potentiometric measurements were performed in a Britton–Robinson buffer (0.04 M boric acid, 0.04 M phosphoric acid and 0.04 M acetic acid with the pH adjusted by the addition of 0.2 M NaOH).

P[6]A (chemical structure is presented in Figure 1) was synthesized at the Department of Organic and Medicinal Chemistry of the Kazan Federal University (Kazan, Russia) as described elsewhere [29]. Briefly, cyclization of 1,4-bis(2-bromoethoxy)benzene was first performed in the presence of methazine sulfonic acid in chloroform at 0 °C, and then hydroxy groups were liberated by treatment with BBr<sub>3</sub>. The structure of P[6]A was confirmed by NMR <sup>1</sup>H and <sup>13</sup>C spectroscopy and by MALDI-TOF mass spectroscopy. Prior to use, synthesized P[6]A was stored under Ar in a frozen state at –20 °C.

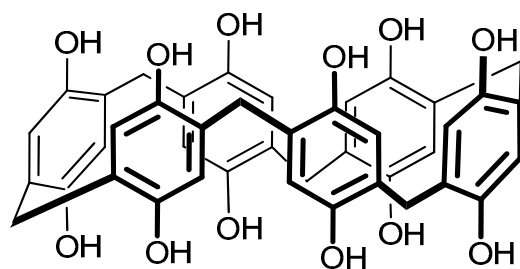


**Figure 1.** Chemical structure of P[6]A used in the investigation.

## 2.2. Apparatus

Electropolymerization of freshly distilled aniline was performed with potentiostat-galvanostat AUTOLAB PGSTAT 302N (Metrohm Autolab, Netherlands) at ambient temperature. A three-electrode cell consisted of the glassy carbon working electrode (GCE, 0.0283 cm<sup>2</sup> geometric surface square), Ni foil auxiliary electrode, and double-junction Ag/AgCl/3 M KCl reference electrode (Metrohm Autolab Cat. No 6.0726.100) was used.

Potentiometric measurements were performed by using digital ionometer Ecotest I-120 (Ecotest, Moscow, Russia) with double-junction Ag/AgCl/3 M KCl reference electrode. The precision of the potential measurement was  $\pm 0.1$  mV.

Surface plasmon resonance (SPR) measurements were performed on the 25 mm BK-7 glass disk covered with the 50 nm thick Au film with the Autolab ESPRIT (Metrohm Autolab b.v., Utrecht, Netherlands) equipped with two-channel cuvette and the 670 nm laser with the p-polarization. An incidence angle shift of the laser beam was recorded as the SPR signal, expressed in millidegrees (m°).

Transmission electron microscopy (TEM) images were obtained with a Hitachi HT7700 Exalens (Tokyo, Japan) microscope at 120 keV. The mixture of P[6]A and CuCl<sub>2</sub>/AgNO<sub>3</sub> was deposited on the formvar/carbon-supported copper grids of 200 mesh.

Scanning electron microscopy (SEM) images of the surface films were obtained with the high-resolution field emission scanning electron microscope Merlin (Carl Zeiss, Dresden, Germany).

Atomic force spectroscopy (AFM) images were obtained with scanning probe microscope Dimension FastScan (Bruker, Mannheim, Germany) in the mode of quantitative nanomechanical mapping with the silicon probes "Bruker scanasyst air", sScan rate 1 Hz.

The content of the Cu in real samples was determined by using microwave plasma-atomic emission spectrometer Agilent MP-AES (Agilent Technologies Australia Pty Ltd., Mulgrave, Australia).

## 2.3. Preparation of Solid-Contact Potentiometric Sensors

The GCE was first mechanically polished and cleaned with acetone and deionized water. Then it was electrochemically cleaned in 0.1 M H<sub>2</sub>SO<sub>4</sub> by repeated cycling of the potential until current stabilization. After that, it was moved to the 0.2 M H<sub>2</sub>SO<sub>4</sub> solution containing 0.07 M aniline. Electropolymerization was performed in direct current mode by repeated cycling of the potential between  $-200$  and  $1100$  mV (10 cycles). In the next steps, 2  $\mu$ L of 1.37 mM P[6]A and 2  $\mu$ L of 1.37 mM 4.0 mM CuCl<sub>2</sub> were alternatively drop-casted on the working electrode surface. Each layer was dried at ambient temperature in air. In most experiments, the upper layer was formed by the P[6]A solution addition. Prior to measurements, the electrode was conditioned in the buffer solution. When not used, the electrodes were stored in dry conditions at 4 °C.

## 2.4. Potentiometric Measurements

All the potentiometric measurements were taken without stirring. After each measurement, the electrode was washed with working buffer to reach steady potential. The concentration of the standard Cu<sup>2+</sup> solution was varied from 10 nM to 10 mM. All the measurements were taken with three individual sensors in triplicate for each one.

The potentiometric selectivity coefficients  $\log K_{Cu,j}^{pot}$  were calculated using the separate solution method (SSM) with 0.01 M solutions of primary and interfering ions [30], in accordance with Equation (1):

$$\log K_{Cu,j}^{pot} = \frac{2F(E_j - E_i)}{2.303RT} + \left(1 - \frac{2}{z_j}\right) \log a_{Cu} \quad (1)$$

where  $E_i$  and  $E_j$  are the potentials;  $a_i$  and  $a_j$  are the activities; and  $z_i = 2$  and  $z_j$  are the charges of the Cu<sup>2+</sup> as the primary ( $i$ ) ion and those of the interfering ions ( $j$ ), respectively. The activities of ions were calculated from the modified form of the Debye–Hückel equation [31].

### 2.5. SPR Measurements

The surface of the golden coating of the SPR chip was first modified with 1 mM MUA dissolved in ethanol under 30 min stirring. Then the surface was rinsed with deionized water. In the case of  $\text{Cu}^{2+}$  deposition, PSS (0.5 mg/mL) and PAA (0.1 mg/mL) were consecutively added to the surface to form a polyelectrolyte complex, as described elsewhere [32]. Between the addition of reactants, the cuvette was washed with deionized water. The most stable coating corresponded to the following underlying complex: MUA-PAA-PSS-PAA. Finally, P[6]A dissolved in aqueous ethanol or methanol (50% *v/v*) and  $\text{CuCl}_2$  dissolved in deionized water were added similarly to that described above for the GCE modification: 100  $\mu\text{L}$  aliquots and 10 min incubation for each portion. The addition of P[6]A and  $\text{Cu}^{2+}$  ions was repeated to form multilayered coatings. A similar protocol was applied for the deposition of the composite P[6]A—Ag<sup>+</sup>. However, owing to lower effect of reactant addition, PDDA (0.1 mg/mL) and PSS (0.1 mg/mL) were used, and the concentration of P[6]A in ethanol was 3.0 mM.

### 2.6. Real Sample Analysis

Bordeaux mixture and “Complivit” pills were first mechanically ground. Then they were dissolved in 50%  $\text{HNO}_3$  and heated to 50–60 °C for 15 min to oxidize the interferences. After that, the solutions were evaporated, and solid residue was dissolved in water, filtered, and pH adjusted to pH = 2.0. Copper vitriol was dissolved in deionized water and filtered, and its pH was adjusted to pH = 2.0 with nitric acid.

## 3. Results

### 3.1. Surface-Layer Assembly

The electropolymerization of aniline on GCE resulted in the formation of the film, exerting electron-to-ion conductivity and providing the reversibility of the potential changes attributed to other components present on the sensor surface. Figure 2 shows typical voltammograms recorded by the repeated cycling of the potential in aniline solution.

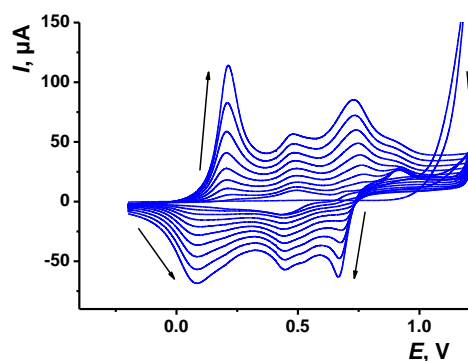


**Figure 2.** Cyclic voltammograms recorded on GCE in 0.2 M  $\text{H}_2\text{SO}_4$  containing 0.07 M aniline, scan rate 50 mV/s. Arrows indicate changes in the peaks with an increasing number of cycles.

The electropolymerization is initiated by the formation of the cation radical at high anodic potential. In consecutive potential cycling, the height of appropriate anodic peak is decreased thanks to the partial shielding of the electrode surface. Three other peak pairs correspond to the redox reactions of the polyaniline forms (leuco-emeraldine, emeraldine salt, and pernigraniline) and of the quinoid byproducts of oxidation [33,34]. They increase within the number of potential cycles, indicating the accumulation of the redox active materials on the electrode. The conditions of the electropolymerization have been specified in our earlier studies concerning the development of potentiometric sensors on the basis of other macrocyclic ionophores [23,35,36]. The use of 10 cycles is a compromise between the requirements of obtaining full coverage of the electrode and the formation of rather thin film with the low barrier of the transfer of counter ions and redox active species. The choice was also confirmed by the metrological assessment of the equilibrium potential,

which showed the lowest deviation (1.1% for six measurements with individual sensors in the range of the cycle variation from 5 to 30). The implementation of P[6]A either on the electrode or in the reaction media did not alter the morphology of the voltammograms but did increase the currents of the pernigraniline-emeraldine salt pair. This is explained by the similarity of the potentials of the oxidation of hydroquinone units of the P[6]A molecules and the polyaniline formed. Owing to the similarity of the redox behavior and possible interferences with  $\text{Cu}^{2+}/\text{Ag}^+$  binding, other experiments were performed with the P[6]A added to the synthesized polyaniline film.

The layer-by-layer deposition of the  $\text{CuCl}_2$  and P[6]A solutions with intermediate washing assumes that their self-assembling was controlled mostly by specific interactions (electrostatic interactions, hydrogen bonding, and chelate complex formation). The quantities of the deposited reactants depended on the characteristics of the underlying surface but not on the amounts of the reagents drop-casted on the electrode. Nevertheless, we assessed the potentiometric response to  $\text{Cu}^{2+}$  obtained for the simplest content of the surface layer (one addition of each component). The aliquot of the P[6]A solution in the range from 2 to 6  $\mu\text{L}$  did not affect the slope of the calibration curve. In the case of higher loading, the deviation of the response increased to 7–8% thanks to the possible formation of supramolecular assemblies and the irregular coverage of the polyaniline surface. The response time insignificantly increased with the volume of the aliquot. For all the assemblies, the reversibility of the redox process remained. It was monitored by measuring the response to the  $\text{Fe}^{3+}$  ions, whose concentration was changed first from a lower value to a higher value and then back (Supplementary Materials, Figure S1). The slope of the calibration curve of  $\text{Fe}^{3+}$  ions was higher in the presence of 0.1 M NaCl than that in acetate buffer (pH 4.5) and than that obtained with polyaniline layer with no P[6]A addition. This confirms the role of P[6]A as a mediator of electron exchange, improving its reversibility. Given the charge of reactants, the repeatability of the signals, and the response time, 2  $\mu\text{L}$  aliquot was chosen for the multilayer coating assembly.

### 3.2. SPR Measurements of the Layer-by-Layer Deposition of P[6]A and $\text{Cu}^{2+}$

The formation of multilayer coatings on the polyaniline electropolymerized on the GCE was confirmed by SPR measurements. For this purpose, a SPR golden chip was modified with the MUC monolayer as a support for the electrostatic accumulation of other reagents. The PAA-PSS-PAA layers were deposited by the consecutive pumping of the reagents through the cell to prevent the possible influence of the MUC terminal carboxylate groups on the P[6]A–metal ions interaction.

Changes in the SPR signal recorded after pumping the P[6]A/ $\text{Cu}^{2+}$  solutions were observed within 200–240 s. After that, a steady-state signal was reached, indicating equilibrium in the transfer of the reactant on the electrode interface. The use of the only reactant, i.e., P[6]A with no  $\text{CuCl}_2$  or vice versa, resulted in rather low adsorption on the underlying surface (Figure 3).

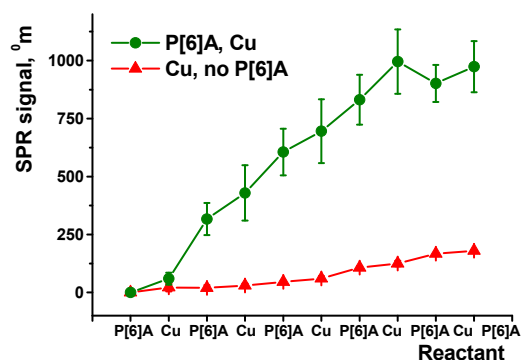


**Figure 3.** The dependence of the SPR signal on the addition of 1.36 mM P[6]A in methanol and 1.36 mM  $\text{CuCl}_2$  in deionized water, SPR chip modified with the MUC, PSS and PAA. Average  $\pm$  s.d. for three replications.

Meanwhile, alternating the addition of both reagents significantly increased the thickness of the surface layer and the appropriate SPR response. This makes it possible to conclude that  $\text{Cu}^{2+}$  ions play a role in bridging ions that promote the deposition of P[6]A via complexation with hydroquinone groups of the macrocycle. The accumulation of the components depended on the solvent used for the P[6]A dissolution (Figure S2). In methanol, the shift of the SPR signal observed or P[6]A— $\text{Cu}^{2+}$  deposition was higher than in ethanol. This can be related to the self-aggregation of the P[6]A molecules that increased the influence of the microenvironment on the SPR phenomenon. Such a process seems inconvenient for assembling the recognition layer because of the lower regularity of its content. Thus, other experiments were performed with the P[6]A dissolved in ethanol.

The obtained results confirm the formation of multilayer composite materials responsible for the response toward the ions implemented in the surface coating.

### 3.3. Scanning Electron and Atomic Force Microscopy

The assembling of the surface layer was confirmed with SEM and AFM images recorded for a glassy carbon electrode modified with polyaniline (Figure 4a,c) and one modified with P[6]A and  $\text{Cu}^{2+}$  (Figure 4b,d). The electropolymerization of aniline resulted in the formation of rather thin film with a sliced structure that consisted of roundish clusters. The deposition of P[6]A molecules and the following treatment with  $\text{Cu}^{2+}$  ions increased the roughness of the layer and increased the size of the particles formed on the polyaniline film. No evidence of the formation of elemental copper or copper oxide particles within the layer were obtained. This confirms the mechanism of chelation with the  $\text{Cu}^{2+}$ -bridging ions binding the macrocycle molecules into the multilayer film.

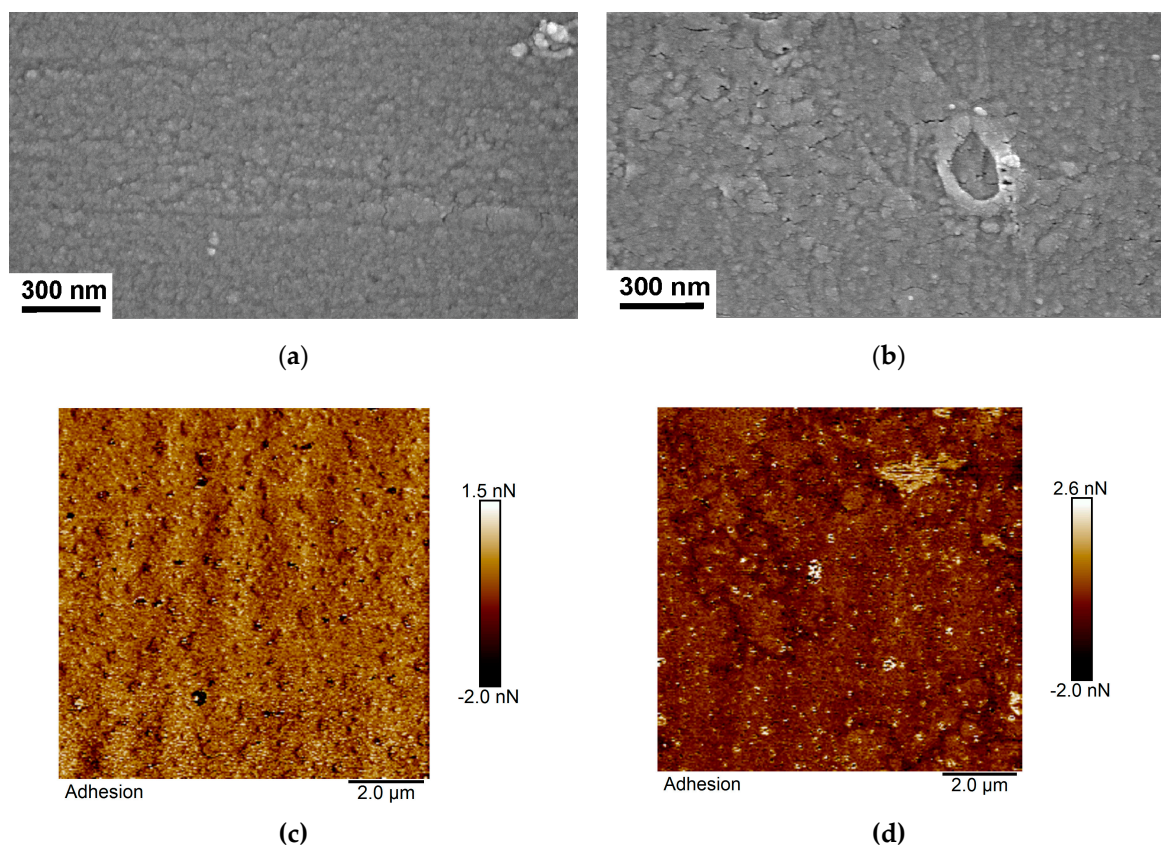


**Figure 4.** SEM (a,b) and AFM (c,d) images of the surface of a glassy carbon electrode modified with polyaniline (a,c) and polyaniline with P[6]A and a  $\text{Cu}^{2+}$  coating (b,d).

### 3.4. Determination of $\text{Cu}^{2+}$ Ions

Copper is a toxic metal that is widely distributed in the environment because of broad industrial applications in the production of electronics and galvanic processes. In addition,  $\text{Cu(II)}$  sulfate is applied in agriculture (copper vitriol and the Bordeaux mixture) as fungicide. Its express determination is highly demanded in hydrochemical analysis waste and fresh water to prevent exhaustive intake into the environment. Although there are many highly sensitive universal instrumentations intended for heavy metal determination, e.g., atomic absorbance spectroscopy and atomic emission spectroscopy (AES), simple and fast methods for the onsite determination of copper content are demanded.

#### 3.4.1. Selection of Measurement Conditions

The performance of the potentiometric sensor consisted of layered P[6]A, and the  $\text{Cu}^{2+}$  layers were assessed with the standard  $\text{CuCl}_2$  solutions. The consecutive addition of the  $\text{Cu}^{2+}$  ions in the concentration range from  $1.0 \mu\text{M}$  to  $10 \text{ mM}$  resulted in a regular increase in the potential. Figure 5 represents the appropriate dependencies obtained for different numbers of the P[6]A— $\text{Cu}^{2+}$  layers.

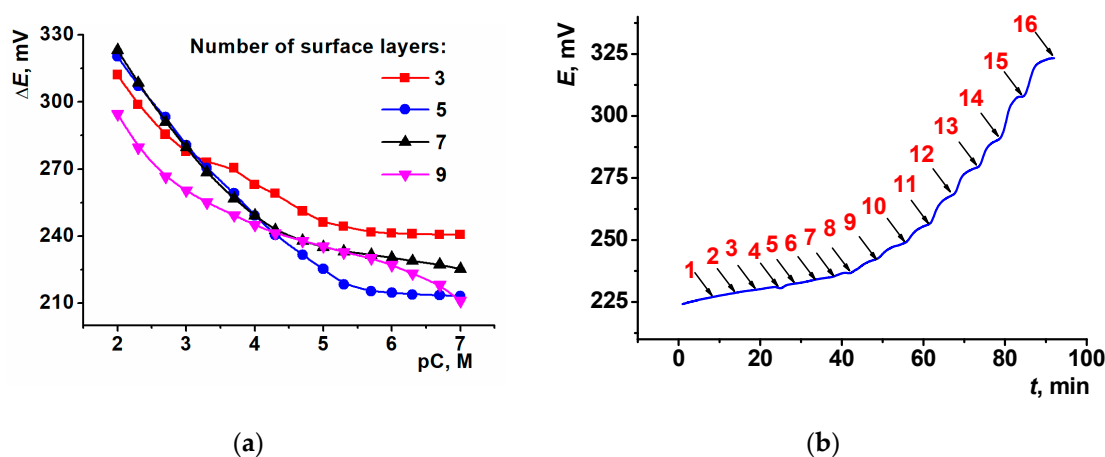


**Figure 5.** (a) Calibration curves of  $\text{Cu}^{2+}$  ions obtained with different numbers of layers deposited on the polyaniline film: P[6]A— $\text{CuCl}_2$ —P[6]A (three layers); (P[6]A— $\text{CuCl}_2$ )<sub>2</sub>—P[6]A (five layers); (P[6]A— $\text{CuCl}_2$ )<sub>3</sub>—P[6]A (7 layers); (P[6]A— $\text{CuCl}_2$ )<sub>4</sub>—P[6]A (nine layers); (b) dynamic response of the potentiometric sensor with seven layers on the addition of  $0.1 \mu\text{M}$ – $10 \text{ mM}$   $\text{CuCl}_2$  solution (concentrations corresponded to red numbers are presented with appropriate numbers in Table S1). Measurements in the presence of  $0.1 \text{ M}$  NaCl.

The analytical characteristics of the  $\text{Cu}^{2+}$  determination are summarized in Table 1. The limit of detection (LOD) was calculated from the  $S/N = 3$  criterion, where  $N$  is the number of experimental points in the linear piece of the calibration curve.

**Table 1.** Analytical characteristics of  $\text{Cu}^{2+}$  determination with potentiometric sensor based on GCE covered with polyaniline and P[6]A— $\text{Cu}^{2+}$  layers. Average results from individual sensors, measurements in triplicate in  $0.1 \text{ M}$  NaCl.

Number of Layers	$E$ , mV = $a + b \times \text{pC}$ , M				Concentration Range, M	LOD, M
	$a \pm \Delta a$	$b \pm \Delta b$	$n$	$R^2$		
3	$344 \pm 5$	$-20.0 \pm 1.5$	10	0.9538	$1 \times 10^{-5}$ – $1 \times 10^{-2}$	$7 \times 10^{-6}$
5	$376 \pm 4$	$-30.7 \pm 1.1$	11	0.9870	$3 \times 10^{-6}$ – $1 \times 10^{-2}$	$2 \times 10^{-6}$
7	$377 \pm 6$	$-29.4 \pm 7.7$	8	0.9759	$2 \times 10^{-4}$ – $1 \times 10^{-2}$	$1 \times 10^{-4}$
9	$293 \pm 3$	$-11.5 \pm 0.7$	11	0.90667	$1 \times 10^{-6}$ – $2 \times 10^{-3}$	$8 \times 10^{-7}$

Only the coatings that consisted of five and seven layers showed that the slopes corresponded to the formal charge of the primary ion. The lower sensitivity for the three-layer-based sensor can be explained by the insufficient coverage of the underlying polyaniline layer and that for the nine-layer-based sensor by the spatial separation of the Cu binding sites and electrode interface.

The best analytical characteristics of the Cu<sup>2+</sup> determination were obtained with the sensors containing an upper P[6]A layer able to form complexes with the metal ions. The attempts to improve the sensor performance by the addition of one more layer that were able to produce the electrostatic accumulation of cationic species (Nafion, PSS) or to stabilize the multilayer assembly (glutaraldehyde) were unsuccessful (Figure 6, Table 2). In the latter case, the slope of the curve decreased against that of double-charged ions thanks to partial involvement of the hydroxyl groups in the reaction with glutaraldehyde and the formation of a denser upper layer influencing the access and distribution of Cu<sup>2+</sup> ions on the electrode interface. The use of six layers with the upper Cu<sup>2+</sup> ions increased the lower quantification limit by one order of magnitude against the sensor with optimal number of layers (five layers, upper P[6]A film).

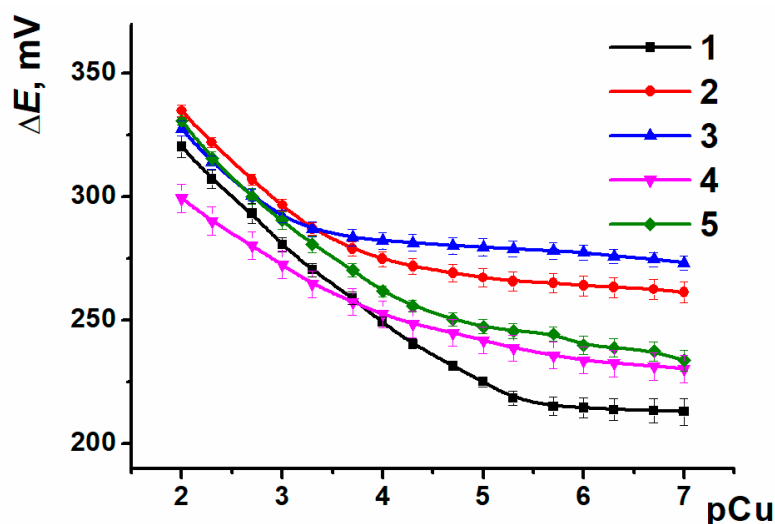


**Figure 6.** Calibration curves of Cu<sup>2+</sup> ions obtained with potentiometric sensor with five layers (1) and an additional upper layer: 2 mg/mL PSS (2), 1% Nafion (3), 3% glutaraldehyde (4), and 4.0 mM CuCl<sub>2</sub> (5).

**Table 2.** Dependence of the analytical characteristics of Cu<sup>2+</sup> determination on the nature of the upper layer, GCE covered with polyaniline and (P[6]A–Cu<sup>2+</sup>)<sub>2</sub>–P[6]A—upper layer. Average results from individual sensors, measurements in triplicate in 0.1 M NaCl.

Nature of Upper Layer <sup>a</sup>	$E, \text{ mV} = a + b \times \text{pC}, \text{ M}$				Concentration Range, M	LOD, M
	$a \pm \Delta a$	$b \pm \Delta b$	$n$	$R^2$		
1	$376 \pm 4$	$-30.7 \pm 1.1$	11	0.9870	$5 \times 10^{-6} - 1 \times 10^{-2}$	$3 \times 10^{-6}$
2	$392 \pm 7$	$-30.4 \pm 2.2$	7	0.9685	$1 \times 10^{-4} - 1 \times 10^{-2}$	$5 \times 10^{-3}$
3	$388 \pm 7$	$-31.3 \pm 2.8$	5	0.9698	$5 \times 10^{-4} - 1 \times 10^{-2}$	$2 \times 10^{-4}$
4	$329 \pm 5$	$-18.1 \pm 1.2$	11	0.9555	$5 \times 10^{-6} - 1 \times 10^{-2}$	$2 \times 10^{-6}$
5	$383 \pm 6$	$-29.7 \pm 1.8$	9	0.9718	$2 \times 10^{-5} - 1 \times 10^{-2}$	$1 \times 10^{-5}$

<sup>a</sup> Layer number corresponds to that described in the caption for Figure 5.

The characteristics of the developed sensor were comparable with other solid-contact potentiometric sensors reported in the literature (Table 3). Meanwhile, they demonstrated a simple and well-reproducible design thanks to the self-assembling of the sensing layer and the minimal use of auxiliary reagents for its assembly.



**Table 3.** Comparison of the performance of the solid-contact potentiometric sensors for Cu<sup>2+</sup> ions determination.

Ionophore/Carrier	Conc. Range, M	LOD, M	Ref.
Bis[2-(hydroxyethylimino)phenolato] Cu(II)/PVC	$1.0 \times 10^{-6}$ – $1.0 \times 10^{-1}$	$8.3 \times 10^{-7}$	[37]
<i>N</i> -hydroxysuccinimide/PVC	$1.0 \times 10^{-4}$ – $1.0 \times 10^{-2}$	$4.4 \times 10^{-6}$	[38]
<i>o</i> -Xylylenebis( <i>N,N</i> -diisobutyldithiocarbamate)/PVC	$1.0 \times 10^{-6}$ – $1.0 \times 10^{-1}$	$4.9 \times 10^{-7}$	[39]
4-(2-hydroxy-benzylideneamino)-5-phenyl-4H-1,2,4-triazole-3-thiol/PVC	$1.0 \times 10^{-6}$ – $1.0 \times 10^{-2}$	-	[40]
Carbon nanotubes, Ag nanoparticles/graphite/Nujol	$5.0 \times 10^{-7}$ – $1.0 \times 10^{-1}$	$2.5 \times 10^{-7}$	[41]
<i>N,N'</i> -bis(5-bromo-2-hydroxy-3-methoxybenzylidene)2-hydroxypropylene-1,3-diamine/PVC on Ag/AgCl	$1.0 \times 10^{-6}$ – $1.0 \times 10^{-2}$	$6.2 \times 10^{-7}$	[42]
Macrocyclic pyrido-pentapeptide derivatives/carbon ink/paper	$5.0 \times 10^{-7}$ – $1.0 \times 10^{-3}$	$8 \times 10^{-8}$	[43]
2-(3-Phenoxy phenyl) propanoic acid/carbon paste	$1.0 \times 10^{-6}$ – $1.0 \times 10^{-2}$	$6.2 \times 10^{-7}$	[44]
P[6]A–Cu <sup>2+</sup> alternating layers/polyaniline/GCE	$3 \times 10^{-6}$ – $1 \times 10^{-2}$	$2 \times 10^{-6}$	This work

In most of the sensors described, a PVC membrane with lipophilic salt was used. Its contents are similar to those commonly applied in the ion-selective electrodes with internal filling. Such sensors have drawbacks related to the leaking of the electrolyte between the membrane and transducer surface and the mechanical braking of the membrane integrity during electrode exploitation. The use of a self-assembling protocol, together with the deposition of a number of alternating layers, minimizes the risk of such complications. The simpler assembly of the sensor also positively affects the cost of the sensor and signal measurement.

#### 3.4.2. Selectivity of the Signal toward Cu<sup>2+</sup> Ions

The potentiometric selectivity of the response toward Cu<sup>2+</sup> ions was assessed by SSM in nonbuffered media and in the presence of 0.01 M HNO<sub>3</sub>. Acidic conditions allowed for suppressing the hydrolysis of the metal salts and improving the redox reversibility of the polyaniline in the sensor assembly. The results are presented in Table 4.

**Table 4.** The potentiometric selectivity,  $\log K_{Cu,j}^{pot} \pm 0.01 \log K_{Cu,j}^{pot}$ , calculated by SSM. Values in the brackets refer to the GCE covered with polyaniline only.

Interfering Ion	H <sub>2</sub> O	HNO <sub>3</sub>	Interfering Ion	H <sub>2</sub> O	HNO <sub>3</sub>
Na <sup>+</sup>	−1.03	−2.30 (−0.30)	Co <sup>2+</sup>	−2.76	−3.53 (−2.53)
K <sup>+</sup>	−1.64	−1.64 (−0.05)	Ni <sup>2+</sup>	−1.72	−2.69 (−2.24)
Mg <sup>2+</sup>	−2.15	−2.65 (−0.45)	Zn <sup>2+</sup>	−1.75	−2.70 (−1.35)
Ca <sup>2+</sup>	−1.91	−2.58 (−0.52)	Cd <sup>2+</sup>	−2.35	−2.63 (−1.50)
Ba <sup>2+</sup>	−1.98	−2.63 (−0.30)	Fe <sup>3+</sup>	7.56	6.54 (3.54)
NH <sub>4</sub> <sup>+</sup>	−2.18	−3.77 (−3.02)	Ag <sup>+</sup>	8.57	7.72 (4.25)

The potentiometric sensor exerted modest selectivity on the signal toward Cu<sup>2+</sup> ions against those of alkali- and alkali-earth metal cations and a higher one toward transient metals. This might have resulted from the difference in cationic interactions involving rather hard cations of alkali- and alkali-earth metal, probably coordinating with oxygen atoms of hydroxyl groups not involved in the Cu<sup>2+</sup> binding within the surface layer. Contrary to that, Co<sup>2+</sup>, Ni<sup>2+</sup>, and Cd<sup>2+</sup> ions compete with the Cu<sup>2+</sup> ions for the P[6]A binding sites so that their influence on the sensor potential is remarkably lower. The transfer of the sensor from the nonbuffered aqueous solutions of the primary and interfering salts to a nitric acid solution did not significantly affect the potentiometric selectivity of 10 nonhydrolyzable cations but increased that for the metals able to hydrolyze in the measurement conditions.

In comparison with the potentiometric selectivity achieved with the GCE covered with polyaniline with no macrocycle, the potentiometric selectivity toward almost all the ions tested increased after the deposition of P[6]A, indicating specific interactions within the surface layer. Changes in the pH of the salt solutions did not significantly alter the potentiometric selectivity, though the absolute signals were shifted to higher values by

an approximately 5–10 mV/pH unit. A minimal pH effect was observed for alkali and alkali-earth metal ions.

The influence of  $\text{Fe}^{3+}$  and  $\text{Ag}^+$  ions is the only exception in that they exerted a higher response against that of  $\text{Cu}^{2+}$  ions. This can be attributed to the influence of the above ions in the redox conversion of the polyaniline affecting its charge and potential. For these two ions, measurements in acidic media resulted in decreases in their influence on the  $\text{Cu}^{2+}$  response against nonbuffered solutions. Probably, the partial hydrolysis of  $\text{Fe}^{3+}$  ions in deionized water promoted its implementation in the surface layer. This is indirectly confirmed by the lower reversibility of the potential changes caused by the addition of  $\text{Fe}^{3+}$  ions contrary to that of  $\text{Cu}^{2+}$  ions. In case of  $\text{Ag}^+$  ions, the interference can be amplified by the deposition of the elemental silver particles, which has been confirmed by the TEM experiments (Figure S3a). Similar images obtained with P[6]A– $\text{Cu}^{2+}$ –P[6]A multilayers did not show the deposition of copper or copper oxides in the macrocycle matrix. In the case of  $\text{Ag}^+$  ions, the following alternating addition of the macrocycle and  $\text{AgNO}_3$  aliquots increased the total layer thickness (see Figure S3b for SPR experiments). Thus, the formation of the Ag nanoparticles within the layer did not suppress the self-assembling of the surface layer. Similar redox reactions with  $\text{Ag}^+$  and  $\text{Cu}^{2+}$  ions were previously described for amperometric sensors containing perhydroxylated thiacalix[5]arene [45] and thiacalix[4]arene derivatives bearing dopamine residues implemented in the  $\text{Ag}^+$  reduction [46]. Although the redox response to the  $\text{Fe}^{3+}$  and  $\text{Cu}^{2+}$  ions was rather high, it was simply eliminated by the addition of 1.0 mM fluoride ions to the samples tested. The additives complex the interfering ions with the formation of a stable complex that did not affect the  $\text{Cu}^{2+}$  ions' response in full range of their concentration.

Thus, the potentiometric sensor based on multilayers of P[6]A and  $\text{Cu}^{2+}$  ions showed remarkable selectivity for  $\text{Cu}^{2+}$  determination in the concentration range sufficient for applications in real sample analyses.

### 3.4.3. Measurement Precision and Storage Conditions

Each solid-contact sensor made it possible to perform up to 30 signal measurements with a measurement-to-measurement repeatability of 3.2% (0.1 mM  $\text{Cu}^{2+}$  ions) without significant changes in the sensitivity. Measurement-to-measurement sensitivity was assessed as 4.5% for a set of three sensors made with the same reagents. Stored in dry conditions at ambient temperature, the potentiometric sensors retained their signal toward the primary ion for more than four months. Intermediately wetting the sensors resulted in a decrease in both storage and operation periods at 1 month and 10 measurements, respectively. Sensors stored in dry conditions were conditioned in 10.0 mM  $\text{HNO}_3$  for 1 h prior to the contact with the  $\text{Cu}^{2+}$  ions.

At a longer storage period, the sensitivity of the signal sharply decreased to about 40–45% of the initial value, probably owing to the deterioration of the multilayer coating caused by the partial oxidation of P[6]A with atmospheric oxygen. Similar investigations performed with a polyaniline-coated electrode made it possible to conclude that at least part of the limitations of the storage period can be related to the aging of the polyaniline layer that loses the reversibility of the redox exchange, which was tested by the measurements of the equilibrium potential in the mixture of the  $[\text{Fe}(\text{CN})_6]^{3-/4-}$  redox pair.

### 3.5. Real Sample Analysis

The performance of the potentiometric sensor was assessed in determination of  $\text{Cu}^{2+}$  ions in two commercial samples containing copper sulfate, i.e., copper vitriol and Bordeaux mixture, and in polyvitamin-mineral drops of “Complivit”. All the samples were treated with nitric acid to remove oxidizable components that could affect the polyaniline redox state and the  $\text{Cu}^{2+}$  signal. The dilution corresponded to the nominal concentrations of  $\text{Cu}^{2+}$  ion, equal to 1.0 mM. Real concentrations were determined with AES by using the same sample treatment. The results of  $\text{Cu}^{2+}$  determination are presented in Table 5.

**Table 5.** The determination of  $\text{Cu}^{2+}$  in real samples with potentiometric sensor based on polyaniline and P[6]A- $\text{Cu}^{2+}$ -layered coating, nominal concentration 1.0 mM.

Sample	$\text{Cu}^{2+}$ Concentration, mM	
	Potentiometric Sensor	AES
Copper vitriol	$0.72 \pm 0.05$	$0.75 \pm 0.01$
Bordeaux mixture	$0.67 \pm 0.04$	$0.70 \pm 0.02$
“Complivit”	$0.95 \pm 0.04$	$0.94 \pm 0.02$

One can see that the results obtained with the developed potentiometric sensor and those with AES by using the same sample treatment did not significantly differ from each other. Despite the presence of many components able to interfere with a  $\text{Cu}^{2+}$  measurement, “Complivit” showed a lower standard deviation and an average value closest to that announced by the manufacturer. The relatively high deviation of the measurement result obtained for  $\text{CuSO}_4$  present in copper vitriol and Bordeaux mixture can be attributed to the inhomogeneous solutions obtained after the dissolution of the solid residues and the presence of mineral-insoluble impurities in the samples tested.

#### 4. Discussion

The use of the layer-by-layer deposition of P[6]A and  $\text{Cu}^{2+}$  made it possible to obtain a regular coating with well-reproducible properties whose potential was sensitive to the  $\text{Cu}^{2+}$  ions present in the solution. The working conditions of the sensor signal measurement are determined to some extent by polyaniline, which plays a role in the transducer with the electron-to-ion conductivity required for the reversibility of the sensor potential. As was shown by the SPR technique, an increased number of drop-casted layers resulted in a regular increase in the coating thickness. Thanks to the self-assembling of the coating, the sensor properties were rather insensitive to the quantities of the reagents added for assembling the surface layer. This can be considered as an advantage of the proposed approach over other solid-contact sensors described in the literature, where PVC membranes and auxiliary reagents were used to establish dense contact of the ionophore with both the solution and the electrode interface. The selectivity of the response to copper ions was comparable with that of other sensors, according to the macrocyclic ionophores [23,25,27,36], and was quite sufficient for the analysis of complex samples such as polyvitamin-mineral pills of “Complivit”. The accuracy of the  $\text{Cu}^{2+}$  determination in copper-containing mineral products applied as fungicides (copper vitriol and Bordeaux mixture) was comparable with the characteristics of the AES method. The choice of acidic conditions for a signal measurement and the interfering effect of  $\text{Ag}^+$  and  $\text{Fe}^{3+}$  ions results from the properties of polyaniline, which shows maximal redox activity in the presence of strong acids and can be oxidized by both above ions. In the case of  $\text{Ag}^+$  ions, interference can be related to the formation of Ag nanoparticles, confirmed by TEM. For  $\text{Cu}^{2+}$  ions, the formation of elemental copper or its oxides was not proven. The latter fact leaves the only mechanism of potentiometric sensitivity toward  $\text{Cu}^{2+}$  ions, i.e., the formation of layered complexes of P[6]A with  $\text{Cu}^{2+}$  as bridging ions involved in chelation by hydroxyl groups of the macrocycles. The specific structure of the P[6]A molecule destroys the intramolecular hydrogen bonds typical for pillar[5]arene [28,45] and simplifies the formation of the supramolecular composites with central metal ions. This is indirectly confirmed by SPR data. The shift in the SPR signal differed depending on the P[6]A or  $\text{Cu}^{2+}$  deposition, indicating their inclusion in separate layers instead of the formation of a homogeneous film.

The possibility of detecting  $\text{Cu}^{2+}$  ions in the range from 10 mM to 1  $\mu\text{M}$  is sufficient for most samples that are commonly tested for the presence of heavy metals, e.g., wastewaters, plant extract, medications, and pesticides. Owing to its simple design, low cost of manufacturing, and the reproducibility of the operational and analytical characteristics, the solid-contact potentiometric sensor based on polyaniline and layered P[6]A and  $\text{Cu}^{2+}$  ions

can find applications in the analysis of copper-containing products used in agriculture and other industries.

**Supplementary Materials:** The following supporting information can be downloaded at <https://www.mdpi.com/article/10.3390/chemosensors11010012/s1>: Figure S1—the dependence of the sensor signal on the concentration of FeCl<sub>3</sub> recorded with the GCE covered with polyaniline and 1.0 mM P[6]A; Figure S2—the dependence of the SPR signal on the addition of 1.0 mM P[6]A in ethanol and methanol and 1.0 mM CuCl<sub>2</sub> in deionized water; Figure S3—(a) TEM image of the P[6]A–Ag<sup>+</sup> mixture, formvar/carbon-supported copper grids of 200 mesh (b) the dependence of the SPR signal on the addition of 1.0 mM P[6]A in ethanol and 1.0 mM AgNO<sub>3</sub> in deionized water; Table S1—concentrations of CuCl<sub>2</sub> solution used for dynamic response assessment (legend to Figure 3b).

**Author Contributions:** Conceptualization, I.S. and G.E.; funding acquisition, G.E.; investigation, M.S., G.G., V.E. and D.S.; methodology, M.S. and A.I.; project administration, G.E.; writing—original draft, G.E. All authors have read and agreed to the published version of the manuscript.

**Funding:** This research was funded by the Russian Science Foundation, grant number 22-13-00070.

**Informed Consent Statement:** Not applicable.

**Conflicts of Interest:** The authors declare no conflict of interest.

## References

1. Cuartero, M.; Crespo, G.A. All-solid-state potentiometric sensors: A new wave for in situ aquatic research. *Curr. Opin. Electrochem.* **2018**, *10*, 98–106. [[CrossRef](#)]
2. Shao, Y.; Ying, Y.; Pong, J. Recent advances in solid-contact ion-selective electrodes: Functional materials, transduction mechanisms, and development trends. *Chem. Soc. Rev.* **2020**, *49*, 4405–4465. [[CrossRef](#)] [[PubMed](#)]
3. Sorvin, M.; Belyakova, S.; Stoikov, I.; Shamagsumova, R.; Evtugyn, G. Solid-contact potentiometric sensors and multisensors based on polyaniline and thiacalixarene receptors for the analysis of some beverages and alcoholic drinks. *Front. Chem.* **2018**, *6*, 134. [[CrossRef](#)] [[PubMed](#)]
4. Zeng, X.; Liu, Y.; Jiang, X.; Waterhouse, G.I.N.; Zhang, Z.; Yu, L. Improving the stability of Pb<sup>2+</sup> ion-selective electrodes by using 3D polyaniline nanowire arrays as the inner solid-contact transducer. *Electrochim. Acta* **2021**, *384*, 138414. [[CrossRef](#)]
5. Hassan, S.S.M.; Kamel, A.H.; Amr, A.E.-G.; Fathy, M.A.; Al-Omar, M.A. Paper strip and ceramic potentiometric platforms modified with nano-sized polyaniline (PANI) for static and hydrodynamic monitoring of chromium in industrial samples. *Molecules* **2020**, *25*, 629. [[CrossRef](#)]
6. Michalska, A.; Wojciechowski, M.; Jedral, W.; Bulska, E.; Maksymiuk, K. Silver and lead all-plastic sensors—Polyaniline vs. poly(3,4-ethylenedioxythiophene) solid contact. *J. Solid-State Electrochem.* **2009**, *13*, 99–106. [[CrossRef](#)]
7. Jaworska, E.; Michalska, A.; Maksymiuk, K. Polypyrrole nanospheres—Electrochemical properties and application as a solid contact in ion-selective electrodes. *Electroanalysis* **2017**, *29*, 123–130. [[CrossRef](#)]
8. De Oliveira, I.A.M.; Risco, D.; Vocanson, F.; Crespo, E.; Teixidor, F.; Zine, N.; Bausells, J.; Samitier, J.; Errachid, A. Sodium ion sensitive microelectrode based on a p-tert-butylcalix[4]arene ethyl ester. *Sens. Actuators B* **2008**, *130*, 295–299. [[CrossRef](#)]
9. Sun, X.X.; Aboul-Enein, H.Y. Influence of anion doped polypyrrole film as ion-to-electron transducer on the response performance of internal solid contact potentiometric sensors. *Instrum. Sci. Technol.* **2009**, *37*, 164–188. [[CrossRef](#)]
10. Yu, S.; Li, F.; Qin, W. An all-solid-state Cd<sup>2+</sup>-selective electrode with a low detection limit. *Sens. Actuators B* **2011**, *155*, 919–922. [[CrossRef](#)]
11. Zhang, L.; Wei, Z.; Liu, P. An all-solid-state NO<sub>3</sub><sup>−</sup> ion-selective electrode with gold nanoparticles solid contact layer and molecularly imprinted polymer membrane. *PLoS ONE* **2020**, *15*, e0240173. [[CrossRef](#)] [[PubMed](#)]
12. Yuan, D.; Anthis, A.H.C.; Afshar, M.G.; Pankratova, N.; Cuartero, M.; Crespo, G.A.; Bakker, E. All-solid-state potentiometric sensors with a multiwalled carbon nanotube inner transducing layer for anion detection in environmental samples. *Anal. Chem.* **2015**, *87*, 8640–8645. [[CrossRef](#)] [[PubMed](#)]
13. Draz, M.E.; Naguib, I.A.; Saad, A.S. Computational ionophore selection during optimization of a portable calixarene based sensor for direct assay of levamisole residues in livestock products. *J. Electroanal. Chem.* **2021**, *897*, 115546. [[CrossRef](#)]
14. Kamel, A.H.; Amr, A.E.-G.E.; Abdalla, N.S.; El-Naggar, M.; Al-Omar, M.A.; Alkahtani, H.M.; Sayed, A.Y.A. Novel solid-state potentiometric sensors using polyaniline (PANI) as a solid-contact transducer for flucarbazone herbicide assessment. *Polymers* **2019**, *11*, 1796. [[CrossRef](#)] [[PubMed](#)]
15. Hussein, L.A.; Magdy, N.; Yamani, H.Z. Stable glycopyrrolonium bromide solid contact ion selective potentiometric sensors using multi-walled carbon nanotubes, polyaniline nanoparticles and polyaniline microparticles as ion-to-electron transducers: A comparative study. *Sens. Actuators B* **2017**, *247*, 436–444. [[CrossRef](#)]
16. Elghobashy, M.R.; Mahmoud, A.M.; Rezk, M.R.; El-Rahman, M.K.A. Strategy for fabrication of stable tramadol solid-contact ion-selective potentiometric sensor based on polyaniline nanoparticles. *J. Electrochem. Soc.* **2014**, *162*, H1–H5. [[CrossRef](#)]

17. Hashemi, F.; Zanganeh, A.R. Electrochemically induced regioregularity of the binding sites of a polyaniline membrane as a powerful approach to produce selective recognition sites for silver ion. *J. Electroanal. Chem.* **2016**, *767*, 24–33. [[CrossRef](#)]
18. Lakard, B.; Magnin, D.; Deschaume, O.; Vanlancker, G.; Glinel, K.; Demoustier-Champagne, S.; Nysten, B.; Bertrand, P.; Yunus, S.; Jonas, A.M. Optimization of the structural parameters of new potentiometric pH and urea sensors based on polyaniline and a polysaccharide coupling layer. *Sens. Actuators B* **2012**, *166*, 794–801. [[CrossRef](#)]
19. Lange, U.; Roznyatovskaya, N.V.; Mirsky, V.M. Conducting polymers in chemical sensors and arrays. *Anal. Chim. Acta* **2008**, *614*, 1–26. [[CrossRef](#)]
20. Ogoshi, T.; Yamagishi, T.-A. Pillararenes: Versatile synthetic receptors for supramolecular chemistry. *Eur. J. Org. Chem.* **2013**, *15*, 2961–2975. [[CrossRef](#)]
21. Sun, J.; Guo, F.; Shi, Q.; Wu, H.; Sun, Y.; Chen, M.; Diao, G. Electrochemical detection of paraquat based on silver nanoparticles/water-soluble pillar[5]arene functionalized graphene oxide modified glassy carbon electrode. *J. Electroanal. Chem.* **2019**, *847*, 113221. [[CrossRef](#)]
22. Dube, L.E.; Patel, B.A.; Fagan-Murphy, A.; Kothur, R.R.; Cragg, P.J. Detection of clinically important cations by a pillar[5]arene modified electrochemical sensor. *Chem. Sens.* **2013**, *3*, 18.
23. Stoikova, E.E.; Sorvin, M.I.; Shurpik, D.N.; Budnikov, H.C.; Stoikov, I.I.; Evtugyn, G.A. Solid-contact potentiometric sensor based on polyaniline and unsubstituted pillar[5]arene. *Electroanalysis* **2015**, *27*, 440–449. [[CrossRef](#)]
24. Kothur, R.R.; Hall, J.; Patel, B.A.; Leong, C.L.; Boutelle, M.G.; Cragg, P.J. A low pH sensor from an esterified pillar[5]arene. *Chem. Commun.* **2014**, *50*, 852–854. [[CrossRef](#)] [[PubMed](#)]
25. Dehabadi, M.; Yemisci, E.; Kursunlu, A.N.; Kirsanov, D. Novel pillar[5]arenes show high cross-sensitivity in PVC-plasticized membrane potentiometric sensors. *Chemosensors* **2022**, *10*, 420. [[CrossRef](#)]
26. Acikbas, Y.; Aksoy, M.; Aksoy, M.; Karaagac, D.; Bastug, E.; Kursunlu, A.N.; Erdogan, M.; Capan, R.; Ozmen, M.; Ersoz, M. Recent progress in pillar[n]arene-based thin films on chemical sensor applications. *J. Incl. Phenom. Macrocycl. Chem.* **2021**, *100*, 39–54. [[CrossRef](#)]
27. Evtugyn, G.A.; Shurpik, D.N.; Stoikov, I.I. Electrochemical sensors and biosensors on the pillar[5]arene platform. *Russ. Chem. Bull.* **2020**, *69*, 859–874. [[CrossRef](#)]
28. Shamagsumova, R.V.; Shurpik, D.N.; Kuzin, Y.I.; Stoikov, I.I.; Rogov, A.M.; Evtugyn, G.A. Pillar[6]arene: Electrochemistry and application in electrochemical (bio)sensors. *J. Electroanal. Chem.* **2022**, *913*, 116281. [[CrossRef](#)]
29. Cao, D.; Kou, Y.; Liang, J.; Chen, Z.; Wang, L.; Meier, H. A facile and efficient preparation of pillararenes and a pillarquinone. *Angew. Chem. Int. Ed.* **2009**, *48*, 9721–9723. [[CrossRef](#)] [[PubMed](#)]
30. Umezawa, Y.; Umezawa, K.; Sato, H. Selectivity coefficients for ion-selective electrodes: Recommended methods for reporting  $K_{A,B}^{pot}$  values (Technical Report). *Pure Appl. Chem.* **1995**, *67*, 507–518. [[CrossRef](#)]
31. Buck, R.P.; Linder, E. Recommendations for nomenclature of ion-selective electrodes (IUPAC Recommendations 1994). *Pure Appl. Chem.* **1994**, *66*, 2527–2536. [[CrossRef](#)]
32. Ivanov, A.N.; Kuzin, Y.I.; Evtugyn, G.A. SPR sensor based on polyelectrolyte complexes with DNA inclusion. *Sens. Actuators B* **2019**, *281*, 574–581. [[CrossRef](#)]
33. Otero, T.F.; Martinez, J.G. Electro-chemo-biomimetics from conducting polymers: Fundamentals, materials, properties and devices. *J. Mater. Chem. B* **2016**, *4*, 2069–2085. [[CrossRef](#)] [[PubMed](#)]
34. Prakash, R. Electrochemistry of polyaniline: Study of the pH effect and electrochromism. *J. Appl. Polymer Sci.* **2002**, *83*, 378–385. [[CrossRef](#)]
35. Evtugyn, G.A.; Shamagsumova, R.V.; Stoikova, E.E.; Sitdikov, R.R.; Stoikov, I.I.; Budnikov, H.C.; Ivanov, A.N.; Antipin, I.S. Potentiometric sensors based on polyaniline and thiacalixarenes for green tea discrimination. *Electroanalysis* **2011**, *23*, 1081–1088. [[CrossRef](#)]
36. Evtugyn, G.A.; Stoikov, I.I.; Belyakova, S.V.; Stoikova, E.E.; Shamagsumova, R.V.; Zhukov, A.Y.; Antipin, I.S.; Budnikov, H.C. Selectivity of solid-contact Ag potentiometric sensors based on thiacalix[4]arene derivatives. *Talanta* **2008**, *76*, 441–447. [[CrossRef](#)]
37. Andac, M.; Coldur, F.; Bilir, S.; Birinci, A.; Demir, S.; Uzun, H. Solid-contact polyvinyl chloride membrane electrode based on the bis[2-(hydroxyethylimino)phenolato]copper(II) complex for trace level determination of copper ions in wastewater. *Can. J. Chem.* **2014**, *92*, 324–328. [[CrossRef](#)]
38. Tutulea-Anastasiu, M.D.; Wilson, D.; del Valle, M.; Schreiner, C.M.; Cretescu, I. A solid-contact ion selective electrode for copper(II) using a succinimide derivative as ionophore. *Sensors* **2013**, *13*, 4367–4377. [[CrossRef](#)]
39. Birinci, A.; Eren, H.; Coldur, F.; Coskun, E.; Andac, M. Rapid determination of trace level copper in tea infusion samples by solid contact ion selective electrode. *J. Food Drug Anal.* **2016**, *24*, 485–492. [[CrossRef](#)]
40. Faridbod, F.; Davarkhah, N.; Beikzadeh, M.; Yekefallah, M.; Rezapour, M.  $\text{Cu}^{2+}$ -selective sensors based on a new ion-carrier and their application for the analysis of copper content of water samples. *Int. J. Electrochem. Sci.* **2017**, *12*, 876–889. [[CrossRef](#)]
41. Ghaedi, M.; Naderi, S.; Montazerzohori, M.; Taghizadeh, F.; Asghari, A. Chemically modified multiwalled carbon nanotube carbon paste electrode for copper determination. *Arab. J. Chem.* **2017**, *10*, S2934–S2943. [[CrossRef](#)]
42. Pietrzak, K.; Wardak, C.; Cristóvão, B. Copper ion-selective electrodes based on newly synthesized salentype Schiff bases and their complexes. *Ionics* **2022**, *28*, 2423–2435. [[CrossRef](#)]

43. Kamel, A.H.; Amr, A.E.-G.E.; Almhizia, A.A.; Elsayed, E.A.; Moustafa, G.O. Low-cost potentiometric paper-based analytical device based on newly synthesized macrocyclic pyrido-pentapeptide derivatives as novel ionophores for point-of-care copper(II) determination. *RSC Adv.* **2021**, *11*, 27174. [[CrossRef](#)] [[PubMed](#)]
44. El Badry, M.M.; Frag, E.Y.; El Brawy, M.H. Rapid potentiometric sensor for determination of Cu(II) ions in food samples. *Microchem. J.* **2021**, *164*, 106065. [[CrossRef](#)]
45. Smolko, V.A.; Shurpik, D.N.; Shamagsumova, R.V.; Porfireva, A.V.; Evtugyn, V.G.; Yakomova, L.S.; Stoikov, I.I.; Evtugyn, G.A. Electrochemical behavior of pillar[5]arene on glassy carbon electrode and its interaction with Cu<sup>2+</sup> and Ag<sup>+</sup> ions. *Electrochim. Acta* **2014**, *147*, 726–734. [[CrossRef](#)]
46. Porfireva, A.V.; Gorbachuk, V.V.; Evtugyn, V.G.; Stoikov, I.I.; Evtugyn, G.A. Glassy carbon electrode modified with silver nanodendrites implemented in polylactide-thiacalix[4]arene copolymer for the electrochemical determination of tryptophan. *Electroanalysis* **2018**, *30*, 641–649. [[CrossRef](#)]

**Disclaimer/Publisher's Note:** The statements, opinions and data contained in all publications are solely those of the individual author(s) and contributor(s) and not of MDPI and/or the editor(s). MDPI and/or the editor(s) disclaim responsibility for any injury to people or property resulting from any ideas, methods, instructions or products referred to in the content.